



# **Nuclear Design of the Magnet Shield for Fusion Reactors**

**M.A. Abdou and C.W. Maynard**

**April 1974**

**UWFDM-98**

Presented at the 1st Topical Meeting on the Technology of Controlled Nuclear Fusion,  
San Diego CA, 14-18 April 1974.

***FUSION TECHNOLOGY INSTITUTE***  
***UNIVERSITY OF WISCONSIN***  
***MADISON WISCONSIN***

# **Nuclear Design of the Magnet Shield for Fusion Reactors**

M.A. Abdou and C.W. Maynard

Fusion Technology Institute  
University of Wisconsin  
1500 Engineering Drive  
Madison, WI 53706

<http://fti.neep.wisc.edu>

April 1974

UWFDM-98

Presented at the 1st Topical Meeting on the Technology of Controlled Nuclear Fusion, San Diego CA,  
14-18 April 1974.

# Nuclear Design of the Magnet Shield for Fusion Reactors

M. A. Abdou  
and  
C. W. Maynard

Nuclear Engineering Department  
University of Wisconsin  
Madison, Wisconsin 53706

FDM 98

Paper presented at the First Topical Meeting on the Technology  
of Controlled Nuclear Fusion held in San Diego - April 14-18, 1974.

## Nuclear Design of the Magnet Shield for Fusion Reactors

M. A. Abdou\* and C. W. Maynard\*

Nuclear Engineering Department, The University of Wisconsin, Madison,  
Wisconsin 53706

### I. Introduction

The blanket of a D-T fusion reactor is required to breed tritium and convert neutron kinetic energy into heat. These requirements are usually satisfied by about 60 to 70 cm of lithium and a reflector of materials such as graphite or stainless steel.<sup>1,2</sup> The energy carried away with the neutrons and photons leaking from such a blanket is roughly 0.1 MeV per initial fusion neutron. Extracting this amount of energy is not crucial from a total plant economics point of view. However, in a fusion reactor utilizing a magnetic confinement scheme, if the neutrons and gammas streaming out of the blanket were allowed to pass directly into the superconducting magnets (which are cryogenically cooled to about 4°K), the total plant power output would not be sufficient to meet the power requirements of the refrigeration system. Hence, the need for a magnet shield is obvious. Here, we present the results of a quantitative study of some important features of the nuclear design of a magnet shield for fusion reactors operating on the D-T cycle and utilizing superconducting magnets for confining the plasma.

The shield is required to perform three major functions: 1- reduce the nuclear radiation heating of the cryogenic coils to a permissible level to be defined shortly, 2- reduce the radiation to the superinsulation which forms a thermal barrier between the magnet and the shield to a level that will allow it to function properly without excessive radiation damage for a satisfactory lifetime (~20 years), and 3- keep the radiation to the magnet to the minimum allowed by a) a tolerable increase in the resistivity of the copper stabilizer and b) the radiation damage to the superconductor.

The energy attenuation required by the refrigeration system can be determined by a compromise between its operating and capital cost, the shield cost, and the increase in the magnet cost if the shield thickness is increased. On the other hand, too large an increase in the resistivity of the copper stabilizer or radiation damage to the superconductor cannot be tolerated during the reactor lifetime. Therefore, a point of prime interest is to see if the attenuation required by the refrigeration system is sufficient to satisfy the stringent requirements of the stabilizer, superconductor, and superinsulation. This is discussed after the optimum refrigeration system requirements are obtained.

In section II, an investigation of possible shielding materials and their attenuation characteristics is carried out. An optimization of the shield thickness from a cost standpoint is contained in section III. The sensitivity of the optimization and the resulting cost per unit power to variations in reactor parameters is also examined. In section IV, the attenuation obtainable with the cost optimized shield is compared to those required by superinsulators and the magnet stabilizer and superconductor.

A considerable fraction of the neutrons leaking from the blanket have kinetic energies above a few MeV. A basic requirement therefore of the shielding material is to have a large attenuation coefficient for high energy neutrons. Inevitably, this has to be a material of moderate or large mass number since inelastic scattering is the most efficient mechanism for reducing the energies of high energy neutrons. Furthermore, light materials such as water, LiH, and lithium have small total cross sections at high energies when compared with heavy materials. Stainless steel and lead have relatively large total cross sections above 3 MeV and the average secondary neutron energy per inelastic collision at 14 MeV is 2.2 and 2.5 MeV in lead and iron, respectively. Both materials are available, relatively inexpensive, and a great deal of knowledge about their characteristics exists. Below the inelastic threshold, however, these materials are no longer effective and a light material should be present. Borated water is efficient and is almost cost free. However, the presence of water in the same system with a high-temperature liquid metal increases significantly the hazard of accidental energy release. Graphite is an alternative choice. In addition, to minimize the gamma emission from radiative capture reactions, it is essential to use a sufficient amount of  $B^{10}$  which has a large  $(n,\alpha)$  cross section for low energy neutrons and is associated with only soft gamma (.5 MeV) emission (compared with a strong line at 7.6 MeV in the capture gamma ray spectrum for iron). Boron carbide ( $B_4C$ ) has been used in control rod applications in fission reactors and seems an excellent choice for neutron moderation and absorption at low energies. With its theoretical density,  $B_4C$  has a high content of  $B^{10}$  of 0.0217 atoms/cm<sup>3</sup>. No significant radioactive decay products are formed in  $B_4C$  irradiation but helium production is large. However, if  $B_4C$  is used in the shield with only 80% of the theoretical density, the swelling problem due to the excessive helium production can be tolerated. Boral (50%  $B_4C$  and 50% Al) is another good choice.

Based on the above discussion, a mixture of stainless steel and boron carbide, or of lead and  $B_4C$ , or a combination of the three materials are reasonable choices and further investigation is needed to find the optimum composition and shield depth for an overall low cost. For this purpose, a fixed composition and configuration of the blanket coupled to a shield for which the parameters are to be varied as shown in figure 1 is considered. The blanket consists of a 1 cm first wall, 42 cm of 95% Li plus 5% structure, 20 cm stainless steel, and 7 cm of 95% Li plus 5% structure. The first wall and blanket structure is niobium in the following calculations but the results in the shield are insensitive to this choice. The extra 7 cm of lithium at the outer face of the reflector region was introduced to meet the cooling requirements of the reflector and inner regions of the shield. As preliminary criteria, the attenuation required in the blanket and shield should be roughly  $10^6$ . This requirement can be satisfied by approximately 70 cm of stainless steel plus boron carbide following the blanket described above. As a starting point, figure 1 in which the blanket is followed by a one meter shield was considered as a reference design for investigating various aspects of the shield design. Six cases for the composition of the shield were considered; 70% SS plus 30%  $B_4C$  (design 114), 70% Pb plus 30%  $B_4C$  (design 115), 35% SS plus 35% Pb plus 30%  $B_4C$  (design 116), 100% SS (design 117), 85% Pb + 15%  $B_4C$  (design 118), and 50% Pb + 50%  $B_4C$  (design 119), where percentages are by volume. Neutronics and photonics calculations were carried out for the six designs. It has been shown<sup>1</sup> that the convergence of the discrete ordinates results for such a system are achieved by  $S_8$  and  $S_4$  overestimates the leakage by 10 to 15%. In order to reduce the cost for these calculations,  $S_4$  was used. The comparison is not significantly affected by the difference between  $S_4$  and  $S_8$ . Cylindrical geometry and the  $P_3$  approximation of the scattering anisotropy were used in all calculations.

The energy leakage,  $L_{TE}$ , is plotted against the distance from the inner boundary of the shield for designs 114 through 117 in fig. 2 and for designs

115, 118, and 119 in figure 3.  $L_{TE}$ , is the sum of the neutron energy leakage,  $L_{nE}$ , and the gamma energy leakage,  $L_{\gamma E}$ , where  $L_{nE}$  is defined in the multigroup representation at any surface of a one-dimensional cylinder as

$$L_{nE}(r) = 2 \pi r \cdot \sum_g E_{ng}(r) J_{ng}(r) \quad (1)$$

where  $J_{ng}$  is the (net) neutron current density at the surface in energy group  $g$ , and  $E_{ng}$  is approximated by the midpoint energy of group  $g$ . Similar definitions apply for gammas with the subscript  $\gamma$  replacing  $n$ . Since the energy deposition in the magnet by neutrons and photons streaming out of the shield increases, in general, with the neutron and photon energies we find it more meaningful in comparing the performance of various shield compositions to compare the "energy" rather than the "number" attenuations.

The results in figures 2 and 3 show that  $L_{TE}$  varies exponentially with the spatial variable,  $r$ , i.e.

$$L_{TE}(r) = L_{TE}(r_0) e^{-\mu_t(r - r_0)} \quad (2)$$

where  $\mu_t$  (with or without the subscript) is the total energy attenuation coefficient. Similar results were found for both the neutron and gamma fluxes i.e.

$$L_{nE}(r) = L_{nE}(r_0) e^{-\mu_n(r - r_0)} \quad (3)$$

$$L_{\gamma E}(r) = L_{\gamma E}(r_0) e^{-\mu_\gamma(r - r_0)} \quad (4)$$

The energy attenuation coefficients  $\mu_n$ ,  $\mu_\gamma$ , and  $\mu_t$  obtained for the six designs discussed above are given in table I. Several conclusions can be reached from examining the attenuation curves of figures 2 and 3 and the energy attenuation coefficients in table I: 1- Comparison of  $L_{TE}$  for designs 114, 115 and 116 shows that stainless steel has considerably better attenuation characteristics than lead if both are mixed with a fair amount of light material. 2- Comparison of  $L_{TE}$  for designs 114 and 117 shows that the presence of  $B_4C$  (or an alternative) is necessary. At the end of a one meter shield the total energy leakage from a 100% stainless steel shield is about two orders of magnitude higher than that from a shield consisting of 70% SS plus 30%  $B_4C$ . This is mainly due to two causes.  $B_4C$  is better than SS at attenuating neutrons below about 2 MeV. In addition, in the absence of  $B^{10}$ , neutrons slowed down eventually get absorbed in radiative capture reactions in stainless steel increasing the gamma energy production. 3- Figure 3 which compares  $L_{TE}$  for 85% Pb + 15%  $B_4C$ , 70% Pb + 30%  $B_4C$ , and 50% Pb + 50%  $B_4C$  shows that increasing the volume percentage of  $B_4C$  to 50% (and probably higher) improves the attenuation considerably. If other light materials such as graphite or water are used, the optimal volume percentages are usually much less (roughly 30%) than that for  $B_4C$ . 4- Although lead is more efficient in attenuating gamma radiation, we found that using stainless steel does not increase the gamma energy leakage,  $L_{\gamma E}$ , appreciably. Furthermore, table I shows that  $\mu_\gamma$  is greater in stainless steel- $B_4C$  than in Pb- $B_4C$  mixtures. These results can be explained as follows. The photons in the shield come primarily from gammas produced by neutron interactions in the shield rather than by penetration from the blanket. Stainless steel attenuates fast neutrons quickly in the first few mean free paths, thus the photons produced have a long distance in which to be absorbed. In addition, the gamma energy leakage in the outer regions is affected most by the gammas produced in these regions. The secondary gamma production in deeper regions of a SS- $B_4C$  shield is significantly lower than that in the same regions of the Pb- $B_4C$  shield.

### III. Optimization of Shield Thickness

Increasing the thickness of the shield increases its cost and the magnet

cost but lowers the refrigeration power<sup>4</sup> requirements. In the following, an optimum thickness is found that minimizes the cost for a given shield composition. For convenience, toroidal reactors are considered when a reference to reactor type is needed. For the most part, however, the results are fairly independent of the reactor type.

The total cost of the reactor as a function of the shield thickness is given by: Total cost = magnet cost + shield cost + refrigeration cost + other fixed costs independent of the shield parameters. Since the reactor is fairly uniform in the toroidal direction the cost can be stated per unit length in the toroidal direction. The above equation can be rewritten as

$$C_T = C_M + C_S + C_R + C_F \quad (5)$$

where the subscripts M, S, R, and F denote magnet, shield, refrigeration, and fixed costs, respectively. All the C's are in dollars per unit length. Expressions for each of these items as a function of the shield parameters are given next.

#### Magnet Cost

The cost of a superconducting magnet is directly related to the stored magnetic energy,  $E_{st}$ . Lubell<sup>3</sup> has stated that the magnet cost is proportional to  $E_{st}^{0.8}$  and Boom<sup>4</sup> has indicated that for special cases it is proportional to  $E_{st}^{1.2}$ . We assume that

$$C_M \propto E_{st}^\zeta / R \quad (6)$$

The stored magnetic energy can be approximated<sup>5</sup> by

$$E_{st} \sim B_t^2 R r_m^2 \quad (7)$$

where  $B_t$  is the toroidal magnetic field at the plasma axis,  $R$  is the major toroidal radius, and  $r_m$  is the inner radius of the magnet and is given by

$$r_m = r_b + t_s \quad (8-a)$$

$$r_b = r_w + t_b \quad (8-b)$$

$r_w$  is the first wall radius,  $t_b$  is the blanket thickness,  $r_b$  is the outer radius of the blanket (inner radius of the shield), and  $t_s$  is the shield thickness which is the variable to be optimized. All lengths are in centimeter units. Assuming  $B_t$  is kept constant, the magnet cost per unit length in the toroidal direction becomes

$$C_M = a_m r_m^{2\zeta} (\$/cm) \quad (9)$$

where  $a_m$  is a magnet cost parameter. A reference value for  $a_m$  is taken from the detailed cost calculations for the UWMAK-I magnet<sup>6</sup> which has an  $r_m$  of 720 cm.

$$a_m = 1.01 \times 10^4 / (720)^{2\zeta} \quad (10)$$

#### Shield Cost

Shield cost is taken to be that of the material in the shield, i.e.

$$C_S = \pi(t_s^2 + 2r_b t_s) \cdot a_s \quad (11)$$

where  $a_s$  is the cost of the shielding material in dollars/cm<sup>3</sup>.

#### Refrigeration Cost

This consists of capital and operating costs. The cost of the completely installed refrigeration system is given<sup>4</sup> by

$$C_i = 6,000 (P_r)^{0.6} \quad (\$/\text{cm}) \quad (12)$$

where  $P_r$  is the thermal load in Watts/cm. The thermal load consists of the nuclear heating load, thermal radiation and conductive losses, in addition to other losses (resistive, lead, etc.). The nuclear heat load,  $P_n$ , can be expressed as

$$P_n = 2\pi r_w W_n e^{-\mu_b t_b} e^{-\mu_s t_s} \quad (13)$$

where  $W_n$  is the neutron wall loading in Watts/cm<sup>2</sup>, and  $\mu_b$  and  $\mu_s$  are the total energy <sup>n</sup> attenuation coefficients (cm<sup>-1</sup>) in the blanket and shield, respectively. The radiation load in typical cases<sup>6</sup> is equal to about  $7.5 \times 10^{-6}$  watt per cm<sup>2</sup> of the surface area of the magnet. We will assume all other losses to be ten times the radiation losses. This is approximately the case<sup>6</sup> and the assumption turns out to be unimportant in the end. Hence, the heat load,  $P_\ell$ , from all losses other than nuclear is given by

$$P_\ell \approx 5 \times 10^{-4} r_m \quad (14)$$

As will be shown later, the optimum shield thickness results in a low refrigeration load and the operating cost is very small. However, it is included here for completeness. Assuming the power cost 10 mills/KWhr and 300 KW(e) are required per KW(t) at 4.2°K, the operating cost for a 20 year plant life can be written as

$$C_0 = 525 P_r \quad (\$/\text{cm}) \quad (15)$$

Allowance can be made in this equation for improvement in efficiency as the operating power increases by replacing  $P_r$  with  $P_r^{0.6}$ .

The total refrigeration cost,  $C_R$ , can now be written as

$$C_R = a_1 [a_2(r_b + t_s) + a_3 e^{-\mu_s t_s}]^{0.6} e^{-\mu_b t_b} \quad (16)$$

where  $a_1 = 6525$ ,  $a_2 = 0.0005$ , and  $a_3 = 2\pi r_w W_n$

#### Optimum Shield Thickness

Using the expressions just derived and minimizing the total cost,  $C_T$  in equation (5) with respect to the shield thickness, the following equation is obtained for the optimum shield thickness,  $t_{s0}$

$$2 a_m (r_b + t_{s0})^{2\zeta - 1} + 2\pi a_s (r_b + t_{s0}) = 0.6 a_1 (a_2 - \mu_s a_3 e^{-\mu_s t_{s0}}) / [a_2 (r_b + t_{s0}) + a_3 e^{-\mu_s t_{s0}}]^{0.4} \quad (17)$$

We have found that less than 1% error in calculating  $t_{s0}$  results if equation 17 is approximated by

$$t_{s0} = \frac{1}{0.6 \mu_s} \text{Log} \left[ \frac{0.6 \mu_s a_r}{2 a_m \zeta (r_b + t_{s0})^{2\zeta - 1} + 2\pi a_s (t_{s0} + r_b)} \right] \quad (18)$$

$$\text{where } a_r = a_1 a_3^{0.6} = 6525 (2\pi r_w W_n e^{-\mu_b t_b})^{0.6} \quad (19)$$

Approximating equation 17 by 18 amounts to assuming that the refrigeration cost,  $C_R$ , is approximated by

$$C_R \approx a_r e^{-0.6 \mu_s t_s} \quad (\$/\text{cm}) \quad (20)$$

and  $a_r$  will be called the refrigeration cost parameter.

### Results

As seen from the above equations, the optimum shield thickness,  $t_{s0}$ , is a function of several parameters such as the wall radius, the neutron wall loading, shielding material cost, etc. A set of typical parameters for a power reactor and present materials cost is given in table II. Table III shows the results for  $t_{s0}$  and individual as well as total cost for various shield compositions based on the reference parameters of table II. Among the compositions considered,  $t_{s0}$  is smallest for 70% SS + 30%  $B_4C$  and largest for 100% SS. The total cost (sum of magnet, shield, and refrigeration costs), however, is smallest for the 50% Pb + 50%  $B_4C$  shield composition. Using this mixture saves about 21 million dollars compared with the 70% SS plus 30%  $B_4C$  composition in the cost of a reactor with minor and major radii of 5 and 13 meters. Furthermore, the energy leakage to the magnet from the optimum lead- $B_4C$  shield is more than an order of magnitude lower than that from the optimum SS- $B_4C$  shield. The total cost for a reactor using 70% Pb + 30%  $B_4C$  is only about one million dollars higher than that for a reactor employing 50% Pb + 50%  $B_4C$ . The last column in table III shows the ratio of  $a_s$  to  $\mu_s$  for the shield compositions under consideration. We call this ratio the "Figure of Merit". It is important to note that this figure of merit is a very good indication of the total cost. In other words, using shield compositions that have lower figures of merit will always result in a lower total cost. Hence, the neutronics design of the magnet shield for a fusion reactor can be made in two steps. First, the shield composition with the lowest figure of merit is selected. Second, the optimum thickness of the shield for this composition is calculated using equation 17 (or eq. 18) using the appropriate reactor and cost parameters.

Sensitivity of  $t_{s0}$  to Reactor Cost Parameters

It can be seen from equation 18 that  $t_{s0}$  varies inversely with  $\mu_s$ ,  $a_m$ ,  $\zeta$ ,  $r_b$ , and  $a_s$  and increases with the refrigeration parameter,  $a_r$ . Except for  $\mu_s$ , the dependence of  $t_{s0}$  on these parameters can be expected to be weak due to the nature of the logarithmic function. Table IV shows the variation of  $t_{s0}$  as well as the total cost for a 50% Pb plus 50%  $B_4C$  shield with several reactor and cost parameters. Case 1 in this table is based on the reference parameters of table II. Case 2 shows that a 100% increase in the magnet cost parameter,  $a_m$ , results in only a 5% decrease in  $t_{s0}$  but results in about a 64% increase in the total cost. In case 3, the cost of  $B_4C$  is increased from 3 \$/kg in the reference case to 10 \$/kg while keeping the price of lead the same. This corresponds to an increase in the shield cost parameter,  $a_s$ , of 113% and results in about 8% decrease in  $t_{s0}$  and a 25% increase in the total cost. The refrigeration cost parameter,  $a_r$ , is increased by 100% in case 4 resulting in a 10% larger  $t_{s0}$  and a 4% greater total cost. Cases 2 to 4 show that  $t_{s0}$  is relatively most sensitive to variations in  $a_r$  and least sensitive to corresponding variations in  $a_m$ . The total cost, however, is most sensitive to changes in the magnet cost.

The optimum shield thickness,  $t_{s0}$ , is plotted as a function of the wall radius,  $r_w$ , in figure 4 (curve a) for the 50% Pb plus 50%  $B_4C$  shield composition. The value of  $t_{s0}$  increases relatively rapidly at small  $r_w$ , passes through a maximum, then decreases again. The relative change in  $t_{s0}$ , however, is small in all cases and is less than 3%. The cost per unit power as a function of  $r_w$  is also plotted in figure 4 (curve b). It decreases as the wall radius increases, passes through a minimum at  $r_w$  of about 4.2 meters, then increases again. It is of interest to note that the minimum cost/power occurs roughly at the same  $r_w$  for which  $t_{s0}$  is a maximum. It should be emphasized here that the neutron wall loading was kept constant (1 MW/m<sup>2</sup>) in deriving the results in figure 4.

Cases 5 to 8 in table IV show the variation of  $t_{s0}$  and the individual as well as the total cost with the neutron wall loading for the 50% Pb plus 50%  $B_4C$  mixture. Figure 5 illustrates this variation for several other compositions. These results show that, for the same composition, the relative change in  $t_{s0}$

is not strongly dependent on the reference wall loading and is about 5 to 7% of the relative change in  $W_n$ . Comparison of the results for cases 5 through 8 in table IV shows that the increase in the total cost as  $W_n$  is raised is modest indicating that higher wall loadings result in lower cost per unit power.

#### IV. Radiation Damage and Attenuation Requirements of the Superinsulator and Magnet

From the above results we can now find out if the attenuation obtained with the optimum shield is sufficient to satisfy the requirements of the stabilizer and superinsulation. Figure 6 shows the response rates for atomic displacement in the stabilizer (copper), dose in superinsulation (mylar), and energy leakage as a function of the shield thickness for a shielding mixture consisting of 50% Pb plus 50%  $B_4C$ . At the optimum thickness (98 cm) for this mixture, the dose in mylar facing the shield is about  $10^6$  rads per gram per year for a neutron wall loading of  $1.0 \text{ MW/m}^2$ . From studies on the effect of radiation on magnet insulations, the mylar can operate under such level of radiation for 20 years without severe deterioration in its dielectric and mechanical properties.<sup>7</sup> A neutron wall loading as high as  $10 \text{ MW/m}^2$  is also acceptable. Figure 6 shows that, for a wall loading of  $1 \text{ MW/m}^2$ , the maximum displacement rate in copper at the optimum shield thickness is about  $10^{-6}$  displacements per atom per year. It is beyond the scope of this study to investigate the radiation damage effects on superconducting and stabilizing materials. However, present knowledge indicates<sup>6</sup> that the stabilizer can be designed to accept levels of radiation about ten times higher than that of figure 6 for 20 years of operation.

Thus, it can be concluded that the energy attenuation implied by cost optimization is sufficient to satisfy the requirements for protecting the superinsulation and magnet from excessive radiation damage.

#### References

1. M. A. Abdou, "Calculational Methods for Nuclear Heating and Neutronics and Photonics Design for CTR Blankets and Shields," Ph.D. Thesis; University Microfilms Inc. 74-8981; also issued as Nuclear Engineering Department, Univ. of Wisconsin reports UWFD-66 and UWFD-67 (July 1973).
2. M. A. Abdou and C. W. Maynard, "Neutronics and Photonics Study of Fusion Reactor Blankets," Proceedings of the First Topical Meeting on the Technology of Controlled Nuclear Fusion, CONF-74040, April 1974 (these proceedings).
3. M. S. Lubell et.al, "Economics of Large Superconducting Toroidal Magnets for Fusion Reactors," ORNL-TM-3927 (1972).
4. W. C. Young, and R. W. Boom, "Materials and Cost Analysis of Constant Tension Magnet Windings for Tokamak Reactors," 4th International Magnet Conference, Brookhaven (Sept. 1972); also R. W. Boom, Univ. of Wisconsin - Private Communication.
5. D. Klein, G. A. Emmert, and T. Yang, "Optimization Considerations in the Design of a Tokamak Reactor," Univ. of Wisconsin report FDM-46 (April 1973).
6. B. Badger et.al., "UWMAK-I, A Wisconsin Toroidal Fusion Reactor Design," University of Wisconsin, Nuclear Engineering Department, UWFD-68 (November 1973).
7. P. A. Sanger, "Irradiation Effects to Insulators and Their Application to UWCTR," Univ. of Wisconsin report FDM 59 (March 1973).

Table I

Neutron, Gamma, and Total Energy Attenuation Coefficients\*  
for Various Shield Compositions

Design ID	114	115	116	117	118	119
Shield Composition (all percentages are by volume)	70% SS + 30% B <sub>4</sub> C	70% Pb + 30% B <sub>4</sub> C	35% Pb + 35% SS + 30% B <sub>4</sub> C	100% SS	85% Pb + 15% B <sub>4</sub> C	50% Pb + 50% B <sub>4</sub> C
Neutron Energy Attenuation Coefficient, $\mu_n$ (cm <sup>-1</sup> )	0.1438	0.1113	0.1282	0.1022	0.0977	0.1161
Gamma Energy Attenuation Coefficient, $\mu_\gamma$ (cm <sup>-1</sup> )	0.1466	0.1160	0.1320	0.0828	0.1008	0.1190
Total Energy Attenuation Coefficient, $\mu_t$ (cm <sup>-1</sup> )	0.1445	0.1113	0.1283	0.0902	0.0976	0.1161

\* obtained by fitting the energy attenuation curves to exponentials (see Text)

Table II  
Values of Reference Parameters for  
Optimization of Shield Thickness

Parameter	Reference Value	Shield Composition (percentages are by volume)	$a_s^+$ (\$/cm <sup>3</sup> )
$\zeta$	0.8	70% SS + 30% B <sub>4</sub> C	$18.7740 \times 10^{-3}$
$r_w$	550.0 cm	70% Pb + 30% B <sub>4</sub> C	$7.0308 \times 10^{-3}$
$r_b$	620.0 cm	35% Pb + 35% SS + 30% B <sub>4</sub> C	$12.9024 \times 10^{-3}$
$w_n$	1.0 MW/m <sup>2</sup>	100% SS	$23.58 \times 10^{-3}$
$\mu_b$	0.0703 cm <sup>-1</sup>	85% Pb + 15% B <sub>4</sub> C	$6.9174 \times 10^{-3}$
$\mu_s$	*	50% Pb + 50% B <sub>4</sub> C	$7.182 \times 10^{-3}$

\*  $\mu_s = \mu_t$  given in table I for various shield compositions

+ based on 0.6, 3.0, and 3.0 \$/kg for Pb, SS, and B<sub>4</sub>C, respectively

Table III  
Optimum Shield Thickness,  $t_{so}$ , and Corresponding  
Cost for Various Shielding Compositions  
(Results based on Reference Parameters of Table II)

Shield Composition	$t_{so}$ (cm)	Magnet Cost*	Shield Cost*	Refrigerator Cost*	Total <sup>+</sup> Cost*	Figure of Merit $a_s/\mu_s$ ( $$/cm^2$ )
70% SS + 30% $B_4C$	73.90	77.73	46.73	9.77	134.2	0.130
70% Pb + 30% $B_4C$	101.73	82.77	24.60	6.64	114.0	0.063
35% Pb + 35% SS + 30% $B_4C$	85.18	79.76	37.34	84.11	125.5	0.101
100% SS	105.52	83.47	85.83	19.61	188.9	0.261
85% Pb + 15% $B_4C$	113.69	84.98	27.29	7.61	119.9	0.071
50% Pb + 50% $B_4C$	98.01	82.09	24.14	6.42	112.7	0.062

\* Cost is in millions of dollars and is based on major toroidal radius of 13 meters.

<sup>+</sup> Sum of magnet, shielding material, and refrigerators cost; other fixed costs (independent of  $t_s$ ) are not included.

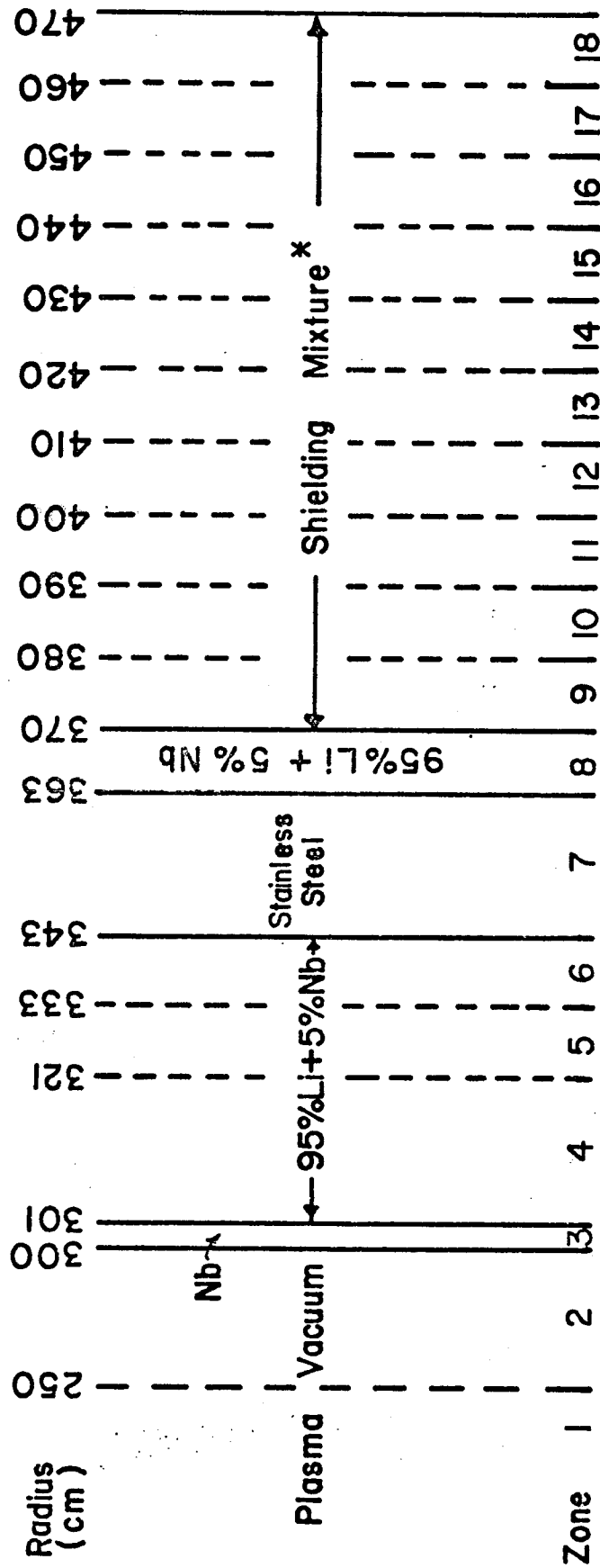
Table IV

Sensitivity of Optimum Shield Thickness,  $t_{so}$ , and  
Corresponding Cost to Variations in Reference Parameters  
for 50% Pb + 50% B<sub>4</sub>C

Case No.	1	2	3	4	5	6	7	8
Variation from Reference Parameters	None (Reference Case)	100% Increase in Magnet Cost Parameter, $a_m$	113% Increase <sup>+</sup> in Shield Cost Parameter, $a_s$	100% Increase in Refrigeration Cost Parameter, $a_r$	$W_n = 0.5 \text{ MW/m}^2$	$W_n = 2 \text{ MW/m}^2$	$W_n = 5 \text{ MW/m}^2$	$W_n = 8 \text{ MW/m}^2$
Optimum Shield Thickness, $t_{so}$ (cm)	98.01	93.16	90.31	107.80	92.14	103.88	111.64	115.63
Magnet Cost*	82.09	162.41	80.69	83.89	81.02	83.17	84.60	85.34
Shield Cost*	24.14	22.87	49.29	26.75	22.60	25.70	27.78	28.86
Refrigeration Cost*	6.42	9.00	10.98	6.49	6.38	6.46	6.52	6.55
Total Cost*	112.7	194.28	140.95	117.13	109.99	115.34	118.9	120.75

\*Cost is in millions of dollars for a major toroidal radius of 13 meters.

<sup>+</sup>Corresponds to 10\$/kg of B<sub>4</sub>C and .6\$/kg of Pb( $a_s$  increased from 0.00718 to 0.0160 \$/ cm<sup>3</sup>)



\* Shielding mixture varies in this series of designs as follows:

Design 114: 70% SS+30% B<sub>4</sub>C, Design 115: 70% Pb + 30% B<sub>4</sub>C

Design 116: 35% SS + 35% Pb + 30% B<sub>4</sub>C, Design 117: 100% SS

Design 118: 85% Pb + 15% B<sub>4</sub>C, Design 119: 50% Pb + 50% B<sub>4</sub>C

Fig. 1 Reference Design for Shield Calculations

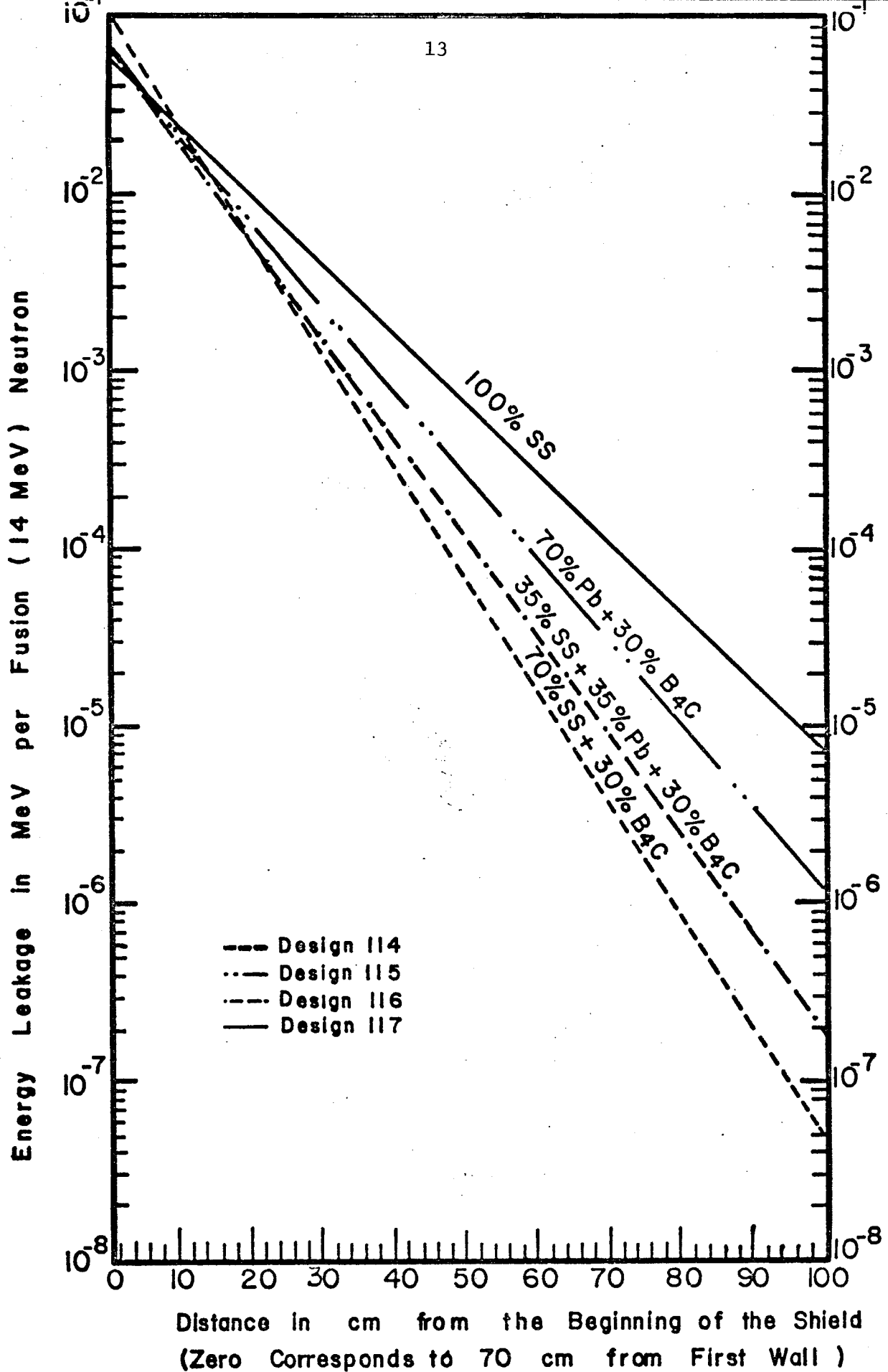


Fig. 2 Energy Leakage Versus Depth in Various Shield Compositions

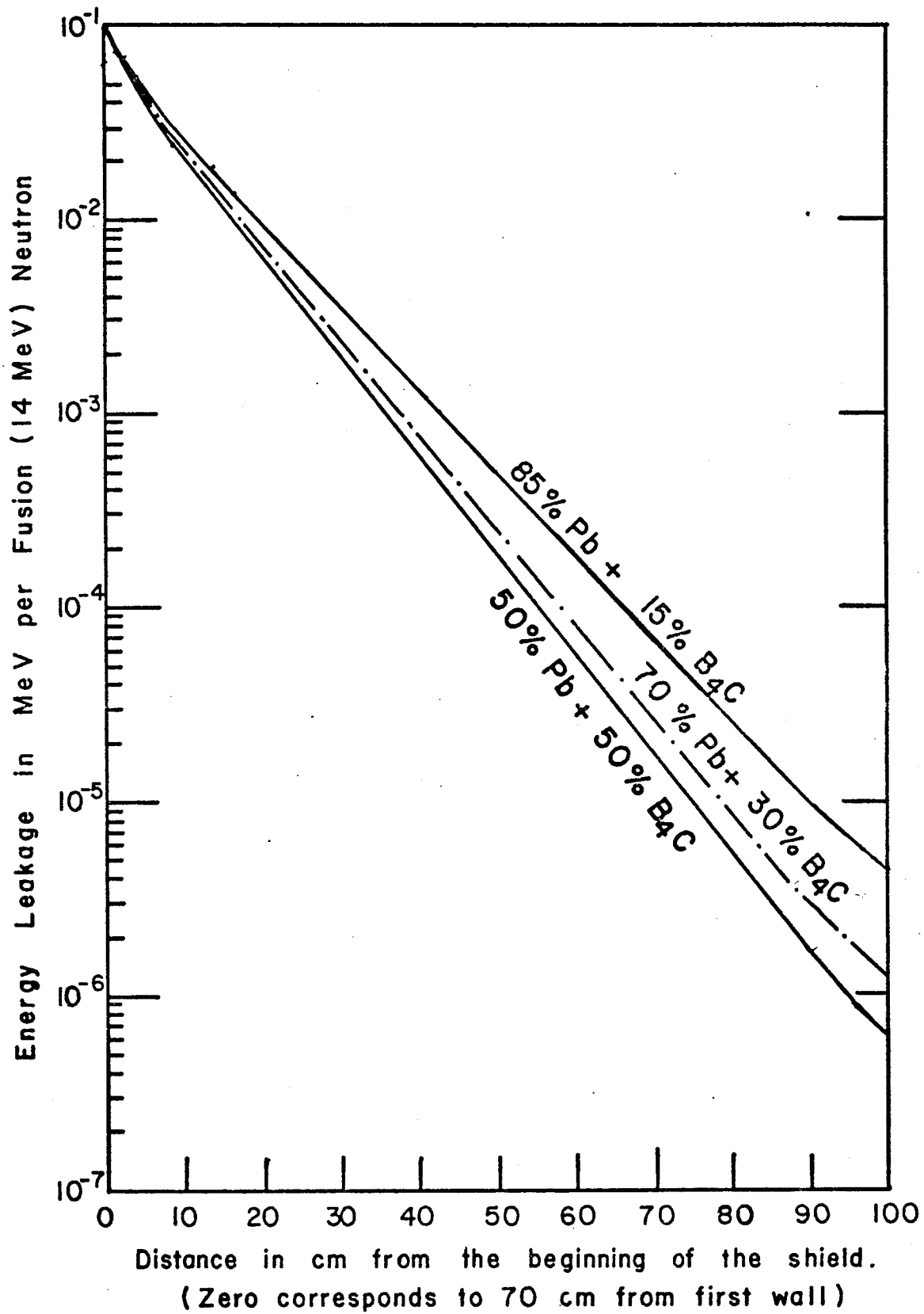


Fig. 3 Effect of Volume Percentages of B<sub>4</sub>C in Pb-B<sub>4</sub>C Mixture on Energy Attenuation

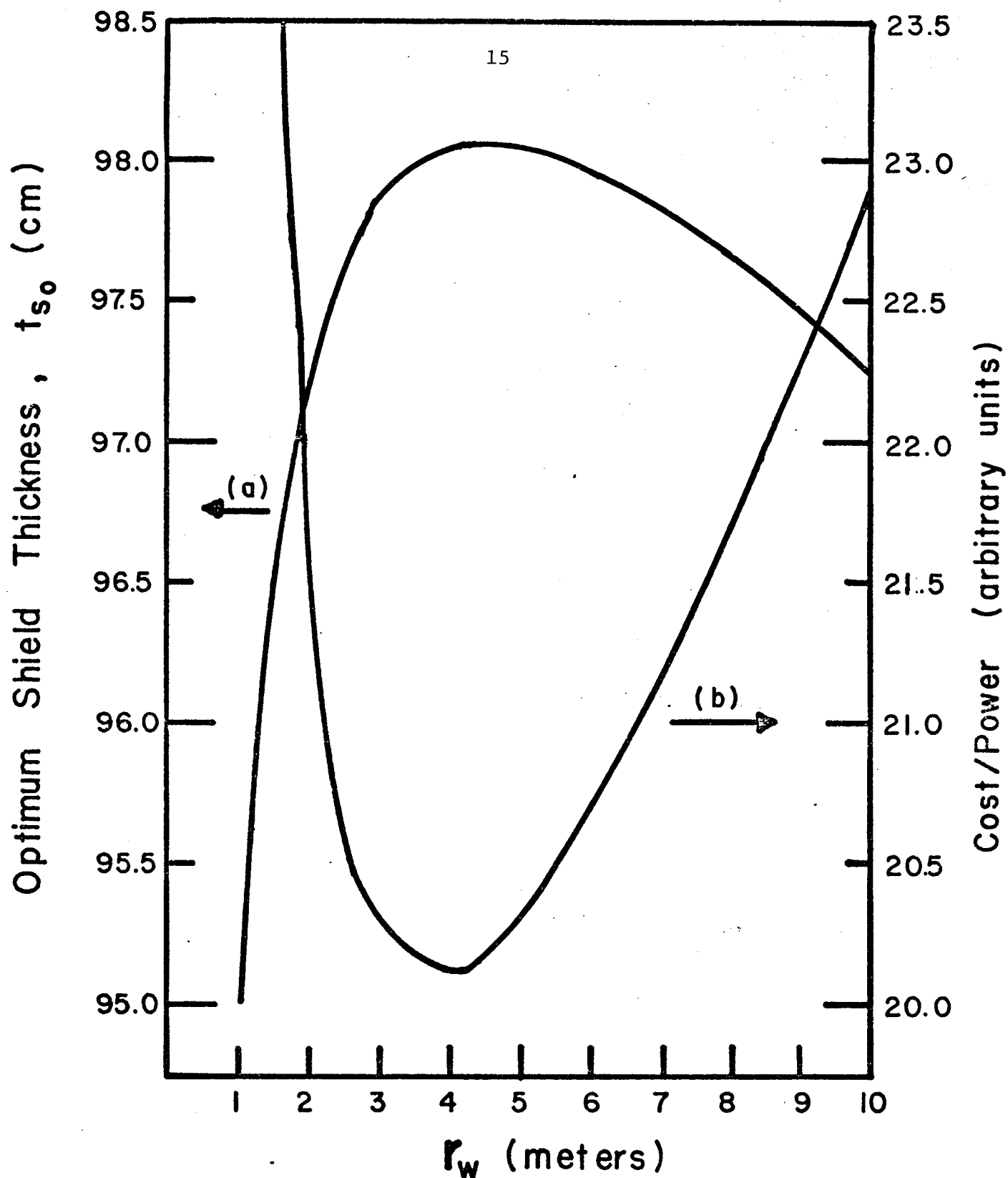


Fig. 4 (a) Optimum shield thickness,  $t_{s0}$ , versus first wall radius,  $r_w$ ; (b) Cost/power (corresponding to  $t_{s0}$ ) versus  $r_w$ . Shielding material is 50% Pb + 50% B<sub>4</sub>C.

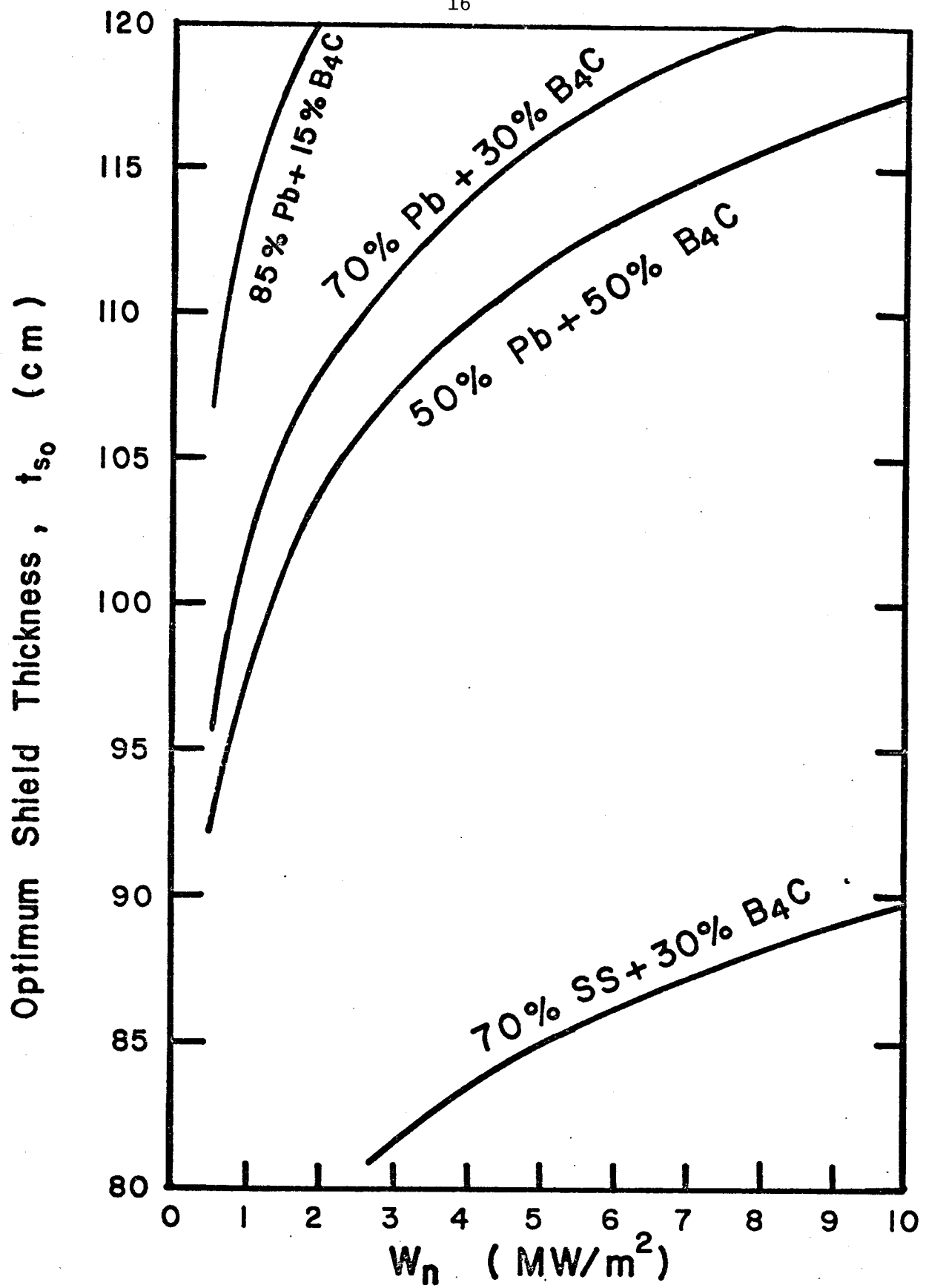


Fig. 5 Variation of optimum shield thickness,  $t_{s_0}$ , with neutron wall loading.

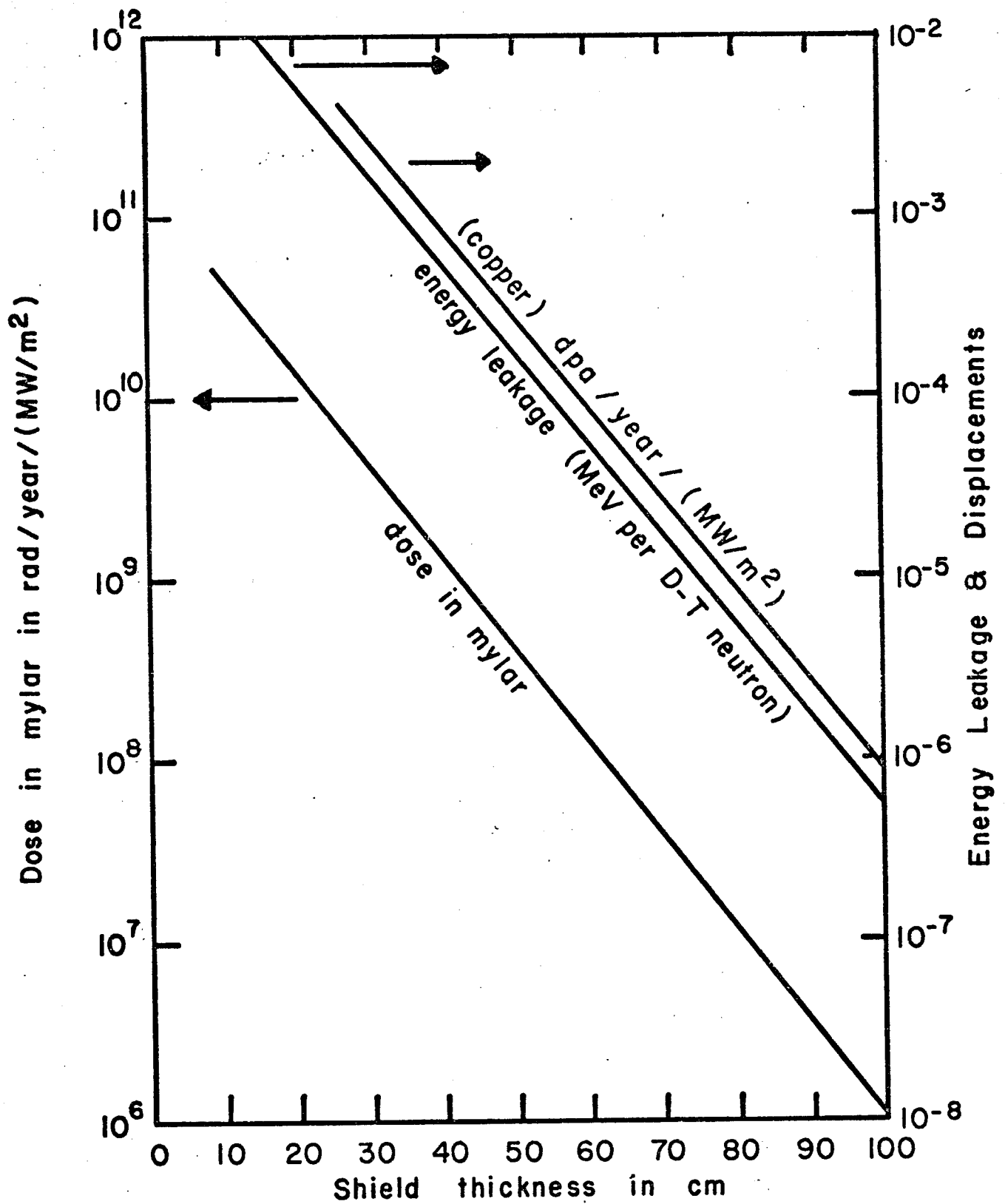


Fig. 6 Atomic displacement in magnet stabilizer(copper), dose in superinsulator(mylar), and energy leakage as a function of magnet shield (50 % Pb + 50% B<sub>4</sub>C) thickness.